Science of the Total Environment 653 (2019) 120–130

Contents lists available at ScienceDirect

Science of the Total Environment

journal homepage: www.elsevier.com/locate/scitotenv

Land pavement depresses photosynthesis in urban trees especially under drought stress

Xu-Ming Wang [a,b], Xiao-Ke Wang [a,b,c,*], Yue-Bo Su [a,b], Hong-Xing Zhang [c]

[a] State Key Laboratory of Urban and Regional Ecology, Research Center for Eco-Environmental Sciences, Chinese Academy of Sciences, Beijing 100085, China
[b] University of Chinese Academy of Sciences, Beijing 100049, China
[c] Beijing Urban Ecosystem Research Station, Chinese Academy of Sciences, Beijing 100085, China

HIGHLIGHTS

- Land pavement inhibited photosynthesis of ginkgo significantly.
- Drought significantly decreased photosynthesis of both ash and ginkgo.
- Greater inhibition of land pavement on photosynthesis of urban trees under drought
- Studying photosynthesis processes helps to explain non-stomatal regulation of tree.

GRAPHICAL ABSTRACT

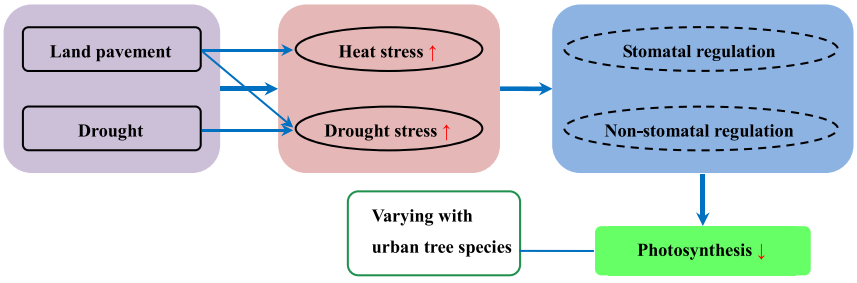

ARTICLE INFO

Article history:
Received 6 August 2018
Received in revised form 18 October 2018
Accepted 20 October 2018
Available online 22 October 2018

Editor: Elena PAOLETTI

Keywords:
Land pavement
Drought
Gas exchange
Chlorophyll fluorescence
Photosynthetic parameter
Urban tree

ABSTRACT

Investigations into the photosynthetic response of urban trees on paved land under drought stress would help to improve the management of trees under rapid urbanization and climate change. An experiment was designed to grow two common greening tree saplings, ash (*Fraxinus chinensis* Roxb.) and ginkgo (*Ginkgo biloba* L.), in environments of both land pavement and drought. The results showed that (1) land pavement increased surface and air temperatures and decreased air humidity as well as net photosynthetic rate (P_n) and photosynthetic capacity (A_{max}) of ginkgo significantly; (2) drought significantly decreased P_n, A_{max} and maximum net photosynthetic rate (P_{nmax}) as well as other photosynthetic parameters of both ash and ginkgo; (3) the negative effects of the combination of land pavement and drought on photosynthetic parameters were more significant than the effects of drought treatment for both ash and ginkgo. This implies that urban trees, especially those growing on land pavements, will confront harsher environments and a greater decline of photosynthesis under the severe and more frequent droughts predicted in the future. Overall, ash showed more tolerance to land pavement and drought than ginkgo, indicating that the selection of tolerant tree species is important for urban planting.

1. Introduction

Trees are an important component of urban green infrastructure that can play an irreplaceable role on improving urban environments (Hagishima, 2018; Sanesi et al., 2016). They can mitigate heat island effects (Edmondson et al., 2016; Leuzinger et al., 2010), alleviate urban waterlogging (Berland et al., 2017; Bian et al., 2017), improve air quality (Escobedo et al., 2011), reduce noise pollution (Margaritis and Kang, 2017), increase carbon sequestration (Weissert et al., 2016), and enhance the aesthetics of the landscape (Rantzoudi and Georgi, 2017). Urban trees can provide a wide range of ecosystem services and are benefit to the health, comfort, and well-being of urban dwellers (Douglas, 2012). Currently, more than half of the global human population live

* Corresponding author at: State Key Laboratory of Urban and Regional Ecology, Research Center for Eco-Environmental Sciences, Chinese Academy of Sciences, Beijing 100085, China.
E-mail address: wangxk@rcees.ac.cn (X.-K. Wang).

https://doi.org/10.1016/j.scitotenv.2018.10.281
0048-9697/

in cities and towns, and the proportion is expected to increase to 70% by 2050 (Edmondson et al., 2012), therefore, the ecosystem services provided by urban trees will become increasingly important for global sustainable development. However, in urban areas, the rapid expansion of various infrastructures for convenient transportation, efficient production, and high-quality living has left few land to planting trees (Kuang et al., 2012). Many trees that are growing in an urban environment are surrounded by artificial pavements such as roads, squares, and parking lots (Weng, 2012), which may create hostile microenvironments for trees via increasing soil and surface temperature (Chen et al., 2016; Yang et al., 2017), reducing water infiltration (Qin et al., 2013), restricting nutrient input (Mullerova et al., 2011), and inhibiting soil–air gas exchange (Balakina et al., 2005). Growing in this unfavorable habitat, urban trees suffer from restricted growth and are even more vulnerable to death, which eventually degrades their ecological functions (Chen et al., 2017a; Mullaney et al., 2015). Previous studies have shown that land pavements or even small patches of ground cover, such as residential yards or driveways, can trigger drought stress, heat stress, and nutrient stress in urban trees (Ghosh et al., 2016; Mueller and Day, 2005) and adversely affect plant growth (Chen et al., 2017a), leaf gas exchanges, including photosynthetic rate, transpiration rate, and stomatal conductance (Song et al., 2015), and other key biochemical parameters (You et al., 2016).

Global climate change is projected to incur warmer, longer, and more frequent droughts in many regions of the world (Breshears et al., 2009). Increasing temperatures and even heat waves resulting from climate change may exacerbate the urban heat island (UHI) effect (Grimm et al., 2008; Savi et al., 2015). Furthermore, due to more evapotranspiration resulting from the enhanced UHI and the less available water in the soil resulting from an extensive impervious surface, drought stress on urban plants could be more serious in the future (Liu and Deng, 2011; Oleson et al., 2013). Studies on the interactions between climate change and UHI/impervious surface on urban trees have been carried out recently (McClung and Ibáñez, 2018; Moser et al., 2017b). However, there is less investigation on whether land pavement would aggravate or alleviate drought stress on urban trees (Savi et al., 2015).

Photosynthesis, the most fundamental and intricate physiological process in green plants (Ashraf and Harris, 2013), is very susceptible to many environmental factors, such as temperature, light intensity, air CO_2 concentration, air humidity, and soil moisture (Ashraf and Harris, 2013). The characteristics of the photosynthetic response to light and CO_2 have been used as an important instrument in elucidating the acclimation of plant photosynthesis process in changing environments (Robredo et al., 2010; Yang et al., 2016a). With the advancement of instrument to measure photosynthesis, more photosynthetic parameters can be measured almost nondestructively in the field and fitted with the curve models of the response of net photosynthetic rate to light and CO_2. From these models, series parameters will be derived to characterize the effects of environmental change on plant photosynthesis (Moualeu-Ngangue et al., 2017; Robredo et al., 2010). Therefore, in this study, a field manipulation experiment was deployed to study the interactive effects of pavement and drought on plant photosynthesis processes, based on measurements of gas exchange parameters, chlorophyll fluorescence parameters, and light and CO_2 response curves. Our aims were to (1) explore whether the land pavement could inhibit photosynthesis and the inhibition would be aggravated under low water supply, (2) explore how the processes of photosynthesis are influenced by drought and land pavement, and (3) explore the differences of photosynthetic response on drought and land pavement in different urban tree species.

2. Materials and methods

2.1. Site description

A field manipulation experiment was conducted in a seed test base at Zhangtou Village, Changping District, a suburb of Beijing, China (40°12′N, 116°08′E). The climate is dominated by a typical temperate continental monsoon, with four distinct seasons. The mean annual temperature is 12.1 °C, the annual sunshine duration is 2684 h, and the frost-free period is ca. 200 days. The mean annual precipitation is 542 mm with the majority of rainfall occurring from June to September (Chen et al., 2017a).

2.2. Experimental design

Our experiment began in March 2016 and ended in September 2017. Ash (*Fraxinus chinensis* Roxb.) and ginkgo (*Ginkgo biloba* L.), widely planted in Beijing as reported in a field survey by Guo et al. (2018), were grown in two types of land cover under two levels of soil moisture.

In March 2016, a piece of cropland was split into two blocks as two types of land cover: one was grassed by creeping bentgrass (*Agrostis stolonifera* L.); another was paved by impermeable bricks (50 cm × 50 cm × 8 cm) (Fig. 1). Each block with a size of 20 m × 15 m was divided into twelve plots for planting two species of trees and two soil moisture levels and three replicas for each tree. On each block, pits with a diameter of 40 cm and depth of 35 cm were dug with a spacing of 2 m × 2 m for laying open-air pots in which trees would be planted. The pot used was a thickened plastic bucket with a top diameter of 33 cm, a bottom diameter of 28 cm, and a height of 33 cm. Three evenly spaced 8 mm-diameter holes were drilled at the bottom of the bucket to ensure a soil–air gas exchange with the outside. Before filling with soil, the pot bottom was covered with nylon net to prevent soil dropping out of the drilled holes. A polyvinyl chloride ring was inserted into each pit to prevent soil sliding laterally, and two small bricks were placed on the bottom of each pit to support the pot so that the soil did not adhere to the pot and the air could circulate freely. Each pot was filled with about 23.5 kg soil that was transferred from the 0–30 cm layer of nearby cropland, sieved by a 5 mm-griddle and mixed evenly. The soil texture was classified as sandy loam. The bulk density was 1.17 g cm^{-3}. The field capacity (FC) was 24.1%. The mass fraction of total carbon, total nitrogen, available phosphorus, and available potassium were 4.63 g kg^{-1}, 0.42 g kg^{-1}, 5.40 mg kg^{-1}, and 57.15 mg kg^{-1}, respectively, and the pH value was 7.87. Two-year-old ash and ginkgo saplings with a mean height of 150.70 cm and 95.28 cm, respectively, and basal diameter of 13.11 mm and 9.84 mm, respectively, were transplanted from the Anguo seedling base, Baoding, Hebei Province, China. One sampling was planted in each pot. To ensure sufficient nutrient supply for the growth of saplings, 20 g of slow-release fertilizer (15% TN, 9% P_2O_5, 12% K_2O, and 2% MgO, Osmocote Exact, Scotts Company, Marysville, OH, USA) was added per pot (Gilbert et al., 2011). Prior to the water control test, all pots were well-watered to guarantee the healthy growth of the plants. On 1 May 2016, we began the control of two soil moisture levels by the weighing method, including the control (85–95% FC) and drought stress (65–75% FC) (Kashiwagi et al., 2015). In 05:30–06:30 (Beijing time, UTC + 8) every morning, the pots were watered to reach the setting weight. If the pot weight exceeded the setting weight because of the rain, we would not water the pots until the weight fell below the setting. In total, there were four treatments deployed: the control (C, 85–95% FC), drought (D, 65–75% FC), pavement (P, 85–95% FC in pavement), and drought + pavement (DP, 65–75% FC in pavement). For each treatment and species, three plots as replicas were randomly arranged. Each plot has four pots (Fig. 1).

2.3. Measurements of gas exchange and chlorophyll fluorescence parameters

From May to September of growing season in 2016 and 2017, gas exchange and chlorophyll fluorescence parameters of the leaf were measured twice a month on sunny windless mornings from 08:30 to 11:30, using a portable photosynthesis analyzer (LI-6400, LI-COR, Lincoln, NE, USA) equipped with a fluorescent leaf chamber. The gas flow rate was set to 500 mmol s^{-1}. The measurements were conducted for six fully

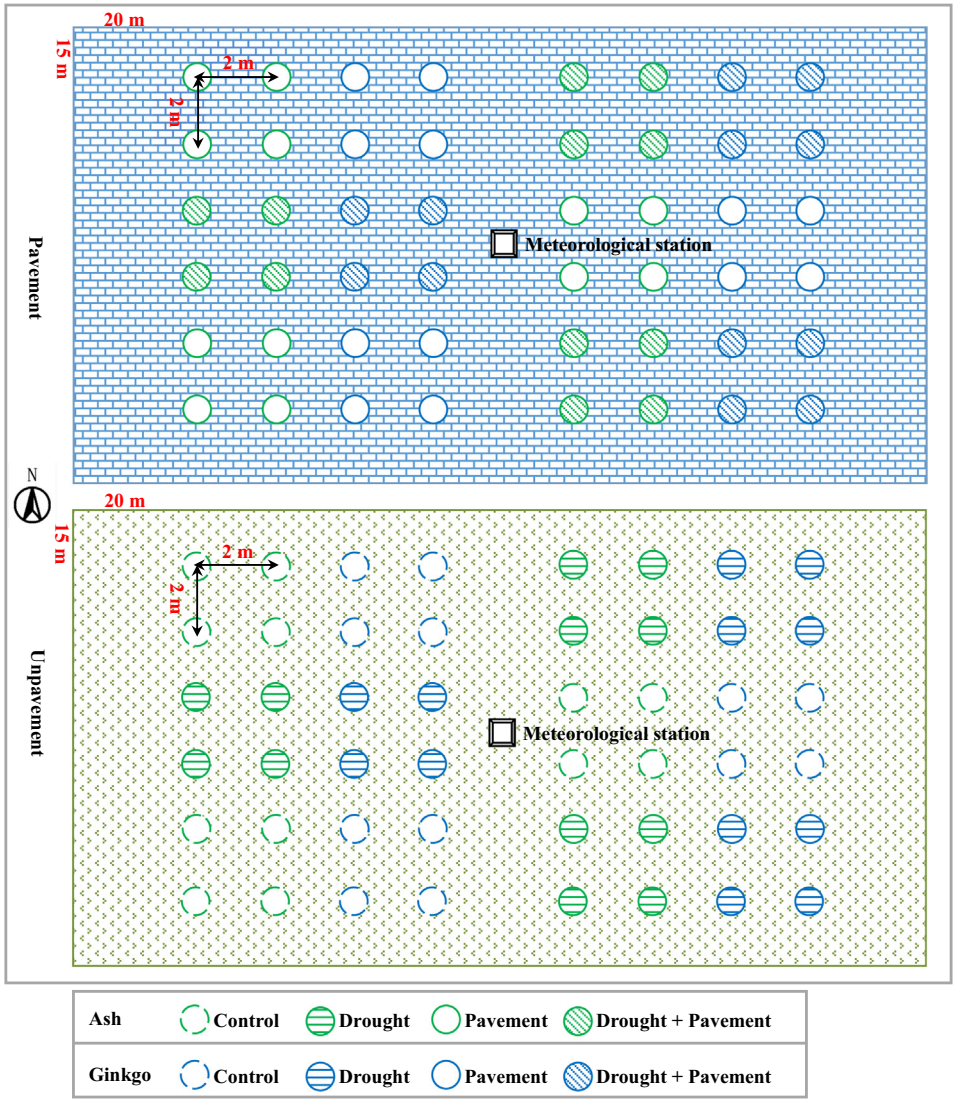

Fig. 1. Layout of the experiment field.

expanded leaves from two trees on each plot under natural light. Three measurements per leaf were recorded at an interval of ca. 30 s.

The following parameters were reported automatically by the instrument: (1) gas exchange parameters: net photosynthetic rate (P_n, μmol m^{-2} s^{-1}), transpiration rate (E, mmol m^{-2} s^{-1}), stomatal conductance (g_s, mol m^{-2} s^{-1}), intercellular CO_2 concentration (C_i, μmol mol^{-1}), and leaf vapor pressure deficit (VPD_l, kPa); (2) chlorophyll fluorescence parameters: minimum fluorescence (F_o), maximum fluorescence (F_m), maximum quantum yield (F_v/F_m), effective quantum yield (Φ_{PSII}), the apparent electron transfer rate (ETR), photochemical quenching parameter (qP), and non-photochemical quenching parameter (NPQ) (Appendix A).

2.4. Measurement of the net photosynthetic rate response to light intensity and CO_2 concentration

The responses of the net photosynthetic rate to light and CO_2 were measured using a portable photosynthesis system (LI-6400, LI-COR, USA) equipped with a fluorescent leaf chamber on a sunny windless morning from 08:30 to 11:30 from May to September in 2016 and 2017. Two fully expanded leaves exposed to the sun at the height of approximately 1.5 m from two trees on each plot were measured. During the measurements, the temperature and relative humidity (RH) of the leaf chamber were set to 25 ± 0.5 °C and 50 ± 5%, respectively. To obtain light-photosynthetic response curves, the leaves were induced with saturation light intensity before the measurements. The reference CO_2 concentration was controlled at 400 μmol mol^{-1} (Danyagri and Dang, 2014) by using CO_2 supplied from a small CO_2 cylinder. The photosynthetic photon flux density (PPFD) gradient consisted of 1800, 1500, 1200, 900, 600, 250, 150, 75, and 0 μmol m^{-2} s^{-1}, and the data acquisition time at each PPFD gradient was 3 min. To obtain CO_2-photosynthetic response curves, the PPFD was set to 1200 μmol m^{-2} s^{-1} (Yang et al., 2016b), and the leaves were induced by the set PPFD for approximately 5 min before measurement. The CO_2 gradient consisted of 400, 300, 200, 100, 50, 400, 600, 800, 1000, 1200, and 1500 μmol mol^{-1} by using CO_2 supplied from a small CO_2 cylinder. The data acquisition time at each CO_2 concentration was 3 min.

Modified rectangular hyperbolic models (see Appendix B) were used to fit the correlations between net photosynthetic rates and light intensities and CO_2 concentrations (Ye, 2010). From the light-photosynthetic response model, we can estimate maximum net photosynthetic rate (P_{nmax}, μmol m^{-2} s^{-1}), light saturation point (I_{sat}, μmol m^{-2} s^{-1}), light compensation point (I_c, μmol m^{-2} s^{-1}), and dark respiration rate (Rd, μmol m^{-2} s^{-1}). From the CO_2-photosynthetic response model, we can estimate photosynthetic capacity (A_{max}, μmol m^{-2} s^{-1}), saturated intercellular CO_2 concentration (C_{isat}, μmol mol^{-1}), CO_2 compensation point (Γ, μmol mol^{-1}), and photorespiration rate (Rp, μmol m^{-2} s^{-1}).

Furthermore, the following biochemical parameters were estimated from the CO_2-photosynthetic response based on a biochemical model (Ethier and Livingston, 2004; Farquhar et al., 1980) (see Appendix B): maximum carboxylation rate (V_{cmax}, μmol m^{-2} s^{-1}) allowed by ribulose 1,5 bisphosphate carboxylase/oxygenase (Rubisco), maximum electron transfer rate (J_{max}, μmol m^{-2} s^{-1}) based on NADPH requirement for ribulose 1,5-bisphosphate (RuBP) regeneration, and triose phosphate utilization rate (TPU, μmol m^{-2} s^{-1}). J_{max}/V_{cmax} was computed as the ratio between J_{max} and V_{cmax}.

2.5. Measurement of environmental factors

In August 2016, a micrometeorological measurement station was installed in the center of each block, equipped with an air temperature and humidity sensor (HMP155, Vaisala, Vantaa, Finland) to measure air temperature (T_a, °C) and RH (%) at the height of 1.5 m, and an infrared thermometer (OPT CS, Optris, Berlin, Germany) to measure land surface temperature (T_s, °C). These measured data were recorded every 10 min by a data acquisition device (CR1000, Campbell, Logan, UT, USA). Daytime and nighttime T_a, RH, and T_s were recorded in 06:00–18:00 and in 00:00–06:00 and 18:00–24:00, respectively. Soil moisture (SM, %) was measured by 10HS soil moisture probes and recorded every 10 min by HOBO RX3001 (Onset, Pocasset, MA, USA).

2.6. Data analysis

To determine the effects of treatment on measured and estimated photosynthetic parameters, we fitted a model with the parameters as the response variables and treatment as the fixed effect while the month was the random effect. If the row or logarithm transformed data were normally distributed (examined by the Shapiro–Wilk test), they were modeled using a general linear mixed model (LMM, function LMER, package LME4). These data included E, C_i, P_{nmax}, I_c, Rd, C_{isat}, Γ, Rp, and J_{max}/V_{cmax} of ash and C_i, NPQ, I_{sat}, I_c, Rd, Γ, and Rp of ginkgo. If they were not normally distributed, they were modeled using a generalized linear mixed model (GLMM, function GLMER, package LME4) fitted to a gamma distribution (with the LOG LINK function). This is suitable for modeling positive continuous response variables resulting in left-skewed distribution (Schule et al., 2017), which is the case for our response variables. These data included P_n, g_s, VPD_l, F_v/F_m, Φ_{PSII}, ETR, qP, NPQ, I_{sat}, A_{max}, V_{cmax}, J_{max}, and TPU of ash and P_n, E, g_s, VPD_l, F_v/F_m, Φ_{PSII}, ETR, qP, P_{nmax}, A_{max}, C_{isat}, V_{cmax}, J_{max}, TPU, and J_{max}/V_{cmax} of ginkgo. We assessed the fitness of the model by calculating conditional R^2 (Nakagawa and Schielzeth, 2013). We used likelihood ratio (LR) tests of a full model against a null model to measure the significance of the treatment effect (Bolker et al., 2009; Jamil et al., 2013). In the case of the fixed effect, Tukey's post hoc pair-wise comparisons (glht function in multcomp library) were used to test for differences between groups (Hothorn et al., 2008). The two-sample t-test was used to identify the differences in air temperature, air RH, land surface temperature between pavement and soil moisture between treatments for each tree species. All analyses were conducted in R v.3.5.0 (R Development Core team, 2018).

3. Results

3.1. Environmental factors

The t-test showed that mean T_a and T_s in the pavement significantly increased by 0.10 °C and 3.07 °C in daytime, respectively, as compared with the control ($P < 0.05$), and a more increase by 0.32 °C and 7.63 °C in nighttime ($P < 0.05$), respectively (Fig. 2a and c). The RH in the pavement was 1.0% and 2.0% lower than that in the control in daytime and nighttime, respectively ($P < 0.05$) (Fig. 2b). When compared with the control, the SM significantly decreased by 2.8%, 0.8%, and 4.1% in D, P, and DP treatments, respectively, for ash ($P < 0.05$) and by 2.7% and 4.0% in D and DP treatments, respectively, for ginkgo ($P < 0.05$) (Fig. 3).

3.2. Gas exchanges and chlorophyll fluorescence

LMM or GLMM showed that the effects of drought (D), pavement (P) and their combination (DP) varied with measured parameters and tree species (Table 1). P_n, E, and g_s decreased significantly in D and DP treatments in comparison to the control for both ash and ginkgo ($P < 0.001$), and the effects of DP treatment were significantly more than that of D ($P < 0.05$). The negative effects of P treatment occurred on P_n and E only for ginkgo ($P < 0.05$) but not for ash; there was no significant effect of P treatment on g_s for both species. C_i in D and DP treatment increased significantly in comparison to the control for ash and ginkgo ($P < 0.05$), and no significant effect of P treatment was found on C_i for both ash and ginkgo. Significantly negative effects on VPD_l occurred in P treatment for both ash and ginkgo ($P < 0.05$) and in DP treatment for ash ($P < 0.001$).

When compared with the control, F_v/F_m decreased significantly in the DP treatment only for ginkgo ($P < 0.001$), Φ_{PSII}, ETR, and qP decreased significantly in D and DP treatment for both ash and ginkgo ($P < 0.05$), and NPQ increased significantly in D and DP treatment for both ash and ginkgo ($P < 0.05$). The negative effects of DP treatment on Φ_{PSII} and ETR were more significant than the effects of D treatment for both ash and ginkgo ($P < 0.05$) and on qP only for ginkgo ($P < 0.05$), the positive effect of DP treatment on NPQ was more significant than that of D only for ash ($P < 0.05$). However, there was no significant effect of P treatment on the above chlorophyll fluorescence parameters for both ash and ginkgo.

According to the Pearson's correlation coefficient, there were significantly positive relationships between P_n and E, g_s, Φ_{PSII}, ETR, and qP and negative between P_n and C_i for both ash and ginkgo ($P < 0.05$). VPD_l and NPQ showed significantly negative influences on the P_n whereas F_v/F_m showed positive influences on the P_n only for ash ($P < 0.05$) (Table 2). Stepwise regression analysis showed that the key factors influencing P_n are E, VPD_l, F_v/F_m, and NPQ for ash and E, C_i, VPD_l, and Φ_{PSII} for ginkgo (Table 3).

3.3. Parameters from light-photosynthetic response model

LMM or GLMM showed that parameters from the light-photosynthetic response model were significantly influenced by drought and its combination with pavement (Table 1). When compared with the control, P_{nmax} decreased significantly in D and DP treatments for both ash and ginkgo ($P < 0.001$), I_{sat} decreased significantly in D and DP treatments for ash ($P < 0.01$) and only in DP for ginkgo ($P < 0.01$), I_c increased significantly in D and DP treatments for ash ($P < 0.001$) and Rd decreased significantly in D ($P < 0.001$), P ($P < 0.001$), and DP ($P < 0.001$) treatments for ginkgo. The effects of DP treatments were significantly higher than D treatment on P_{nmax} for both ash and ginkgo ($P < 0.05$) and on Rd only for ginkgo ($P < 0.05$).

3.4. Parameters from CO_2-photosynthetic response model

LMM or GLMM showed that parameters from CO_2-photosynthetic response model were significantly influenced by drought, pavement and their combination (Table 1). When compared with the control, A_{max}, Rp, V_{cmax}, J_{max}, and TPU decreased significantly in D and DP treatments for both ash and ginkgo ($P < 0.001$), and Γ increased significantly in D and DP treatment for both ash and ginkgo ($P < 0.001$), C_{isat} decreased significantly in D treatment for ginkgo ($P < 0.01$), and J_{max}/V_{cmax} increased significantly in the P ($P < 0.001$) and DP ($P < 0.001$) for ginkgo. The effects of DP treatments were significantly higher than D treatment on A_{max}, Rp, V_{cmax}, J_{max}, and TPU for ash ($P < 0.05$) and on A_{max}, V_{cmax}, and TPU for ginkgo ($P < 0.05$). The negative effects of P treatment on A_{max} and V_{cmax} were significant only for ginkgo ($P < 0.001$).

Fig. 2. Daily mean values of air temperature (a), relative humidity (b) and surface temperature (c) in daytime (06:00–18:00) and nighttime (00:00–06:00 and 18:00–24:00) in the control and pavement observed from 11 August to 30 September 2016 and from 1 April to 25 September 2017.

4. Discussion

4.1. Effects of land pavement on micrometeorology

We observed the pavement significantly increased T_a and T_s and decreased RH in comparison to the control in daytime and more in nighttime (Fig. 2). These influences of pavement on micrometeorology were also found in many previous studies carried out in the field or by simulation experiments (Kjelgren and Montague, 1998; Moser et al., 2017a; Mueller and Day, 2005). Song et al. (2015) reported impervious pavements increased air temperature and decreased air RH in an in-situ experiment in a community in Beijing. Chen et al. (2017a) carried out a simulation experiment by laying impervious and pervious pavements to investigate the physiological responses of common urban trees growing on them and found a significant increase of surface temperature in impervious pavement and a greater increase in pervious pavement. In our study, the pavement material was gray brick with lower thermal capacity than land growing grass, which likely explains the higher surface temperatures and the slight increase of air temperatures in daytime (Kjelgren and Montague, 1998). In nighttime a greater difference in temperature occurred between the

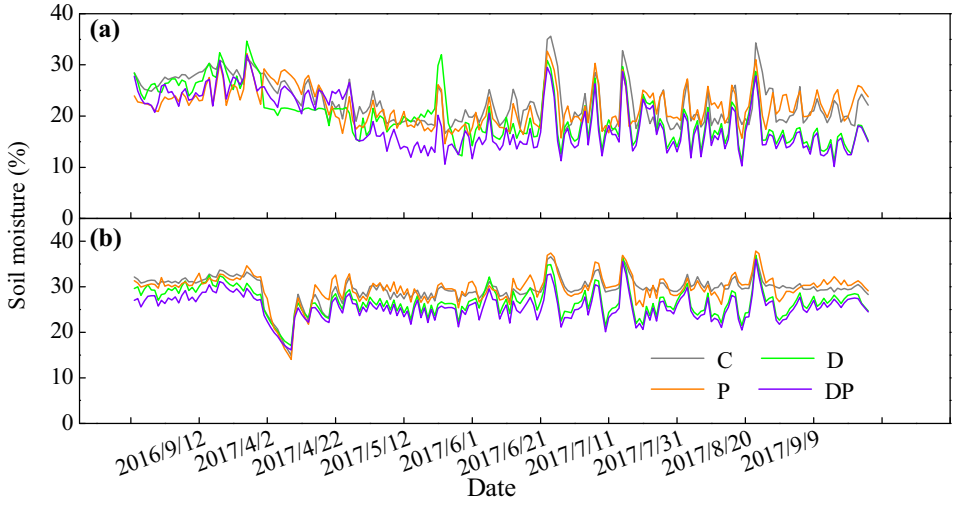

Fig. 3. Daily mean values of soil moisture (%) of different treatments (C: Control, D: Drought, P: Pavement, and DP: Drought + Pavement) in ash (a) and ginkgo (b) observed from 24 August to 30 September 2016 and from 1 April to 25 September 2017.

Table 1
Overall effect of treatments on measured and estimated parameters of ash and ginkgo modeled by general linear mixed model (LMM) or generalized linear mixed model (GLMM), and performance of these parameters in different treatments (D: Drought, P: Pavement, and DP: Drought + Pavement).

Tree species	Parameter	$R^2_{(c)}$	χ^2	*P*	D	P	DP
Ash	P_n	0.46	156.95	<0.001	**−0.41** b	0.01 a	**−0.64** c
	E	0.61	127.07	<0.001	**−0.29** b	−0.02 a	**−0.54** c
	g_s	0.48	113.86	<0.001	**−0.34** b	0.02 a	**−0.46** b
	C_i	0.54	44.16	<0.001	**12.60** b	−1.88 c	**29.47** a
	VPD_l	0.35	16.63	<0.001	−0.03 a	**−0.05** a	**−0.08** a
	F_v/F_m	0.08	7.48	0.058	0.0005 a	−0.005 a	−0.01 a
	Φ_{PSII}	0.25	33.35	<0.001	**−0.10** a	−0.04 a	**−0.23** b
	ETR	0.26	46.53	<0.001	**−0.13** a	−0.05 a	**−0.26** b
	qP	0.18	25.38	<0.001	**−0.09** b	−0.02 a	**−0.12** b
	NPQ	0.22	48.38	<0.001	**0.11** b	0.05 b	**0.19** a
	P_{nmax}	0.87	165.10	<0.001	**−0.52** b	−0.05 a	**−0.72** c
	I_{sat}	0.26	19.82	<0.001	**−0.11** b	−0.004 a	**−0.15** b
	I_c	0.66	85.70	<0.001	**0.53** a	−0.0001 b	**0.54** a
	*R*d	0.51	2.49	0.477	−0.09 a	−0.002 a	−0.18 a
	A_{max}	0.65	94.76	<0.001	**−0.62** b	−0.004 a	**−1.03** c
	C_{isat}	0.29	0.12	0.990	−13.44 a	−8.33 a	−13.32 a
	Γ	0.59	58.05	<0.001	**0.29** a	0.04 b	**0.40** a
	*R*p	0.65	63.32	<0.001	**−0.40** b	0.08 a	**−0.74** c
	V_{cmax}	0.68	102.01	<0.001	**−0.59** b	0.01 a	**−0.97** c
	J_{max}	0.67	97.39	<0.001	**−0.55** b	0.03 a	**−0.97** c
	TPU	0.62	81.13	<0.001	**−0.55** b	−0.01 a	**−0.89** c
	J_{max}/V_{cmax}	0.29	4.00	0.261	0.03 a	0.02 a	0.004 a
Ginkgo	P_n	0.38	113.38	<0.001	**−0.35** b	**−0.10** a	**−0.51** c
	E	0.22	62.95	<0.001	**−0.18** a	**−0.15** a	**−0.37** b
	g_s	0.20	54.58	<0.001	**−0.18** a	−0.08 a	**−0.35** b
	C_i	0.46	41.87	<0.001	**22.30** b	7.86 a	**30.50** b
	VPD_l	0.24	13.56	0.004	0.03 a	**−0.04** b	−0.02 ab
	F_v/F_m	0.12	15.97	0.001	−0.01 ab	−0.001 a	**−0.03** b
	Φ_{PSII}	0.34	94.63	<0.001	**−0.11** b	−0.04 a	**−0.27** c
	ETR	0.30	93.73	<0.001	**−0.11** b	−0.03 a	**−0.27** c
	qP	0.25	69.93	<0.001	**−0.05** a	−0.04 a	**−0.17** b
	NPQ	0.47	23.53	<0.001	**0.08** a	−0.000 b	**0.12** a
	P_{nmax}	0.75	140.79	<0.001	**−0.44** b	−0.10 a	**−0.72** c
	I_{sat}	0.21	14.68	0.002	−77.98 ab	21.12 a	**−142.30** b
	I_c	0.58	1.32	0.725	0.03 a	−0.04 b	−0.06 a
	*R*d	0.56	74.97	<0.001	**−0.76** b	**−0.43** a	**−1.19** c
	A_{max}	0.59	45.34	<0.001	**−0.28** b	**−0.06** a	**−0.48** c
	C_{isat}	0.29	10.24	0.017	**−0.12** a	−0.03 a	−0.06 a
	Γ	0.59	34.18	<0.001	**0.16** a	−0.03 b	**0.18** a
	*R*p	0.60	29.72	<0.001	**−1.43** b	−0.48 a	**−1.80** b
	V_{cmax}	0.55	38.70	<0.001	**−0.26** b	**−0.04** a	**−0.41** c
	J_{max}	0.56	39.56	<0.001	**−0.26** b	−0.01 a	**−0.38** b
	TPU	0.56	41.43	<0.001	**−0.23** b	−0.04 a	**−0.42** c
	J_{max}/V_{cmax}	0.25	9.97	0.019	0.002 a	**0.03** a	**0.03** a

$R^2_{(c)}$ means conditional R^2 calculated referencing Nakagawa and Schielzeth (2013). Data are the estimates of corresponding treatments relative to the control according to the Tukey's post hoc tests from the models, values significantly different from the controls are shown in bold ($P < 0.05$). Different lowercase letters denote significant differences between different groups at $P < 0.05$. The abbreviations of parameters are shown in Appendix A.

pavement and the control because the control was covered by grasses whose evapotranspiration could cause cooling effect. Also because of grass evapotranspiration that could release moisture into air, air RH above the control was higher than that above pavement.

4.2. Effects of land pavement on photosynthesis

Land pavement inhibits the photosynthesis of urban trees which was confirmed by several recent studies (Chen et al., 2017b; Mullaney et al., 2015; Song et al., 2015). Our study conclusively demonstrated that land pavement (P treatment) resulted in a significant reduction in P_n and A_{max} of ginkgo, which represent the maximum photosynthetic capacity of leaves (Table 1). The decrease of A_{max} of ginkgo may be due to the reduction of the photosynthetic enzyme activity deduced from the decline of V_{cmax}. Previous findings suggested that land pavements can trigger drought, heat, and nutrient stress on urban trees growing on them (Ghosh et al., 2016; Mueller and Day, 2005). In particular, a higher temperature and a lower availability of water are often reported for trees on land pavement (Chen et al., 2017b; Song et al., 2015). In the field, it is very difficult to distinguish the individual effect of temperature from water because a rise of temperature could increase the water demand of a plant and cause drought stress, or a water shortage can reduce transpiration, raise temperate, and cause heat stress. In this experiment, we found that in the impervious pavement, surface and air temperature increased while humidity decreased (Fig. 2), which would affect tree photosynthesis. From these results, we cannot infer which of drought and hot is the major contributor to the reduction in P_n for ginkgo. The following discussion on the combing effects of drought and pavement could help us to understand the role of drought in influencing the effect of land pavement on P_n. We did not find significant changes in P_n, P_{nmax}, and A_{max} for ash in the P treatment (Table 1) even though it provided an environment with a higher temperature, lower air humidity but limited reduction in soil moisture as compared with the control, indicating that by maintaining adequate soil moisture the photosynthesis of certain trees on pavements would not be significantly affected.

4.3. Effects of drought and its combination with pavement on photosynthesis

Drought stress can adversely affect the photosynthesis of trees. In this study, the P_n, P_{nmax}, and A_{max} significantly decreased in drought (D treatment) for both ash and ginkgo (Table 1). A significantly greater down-regulation of P_n, P_{nmax}, and A_{max} in DP than in D (Table 1) indicated that land pavement could aggravate the reduction of photosynthesis under drought stress. This also indicated that under the prediction of more frequent and intensive heat waves and severe droughts (Reichstein et al., 2013), urban trees, especially those growing on land pavement, will confront a harsher pavement environment and a greater decline in photosynthesis and growth. These results highlight the crucial importance of regular watering to avoid drought stress for urban trees especially growing on land pavement.

The decrease of photosynthetic rate under environmental stress is mainly attributed to three regulations, which include stomatal regulation (disruption in the CO_2 supply caused by stomatal closure), non-stomatal regulation (decrease in Rubisco activity, CO_2 availability in the chloroplast, and PSII photochemistry efficiency, etc.), and a combination of these two regulations (Chaves et al., 2009; Xu et al., 2014). In general, under mild or moderate drought, the first option for plants is to close the stomata, while under severe and/or chronic drought, the limited photosynthesis is mainly due to a decline in Rubisco (Farooq et al., 2009). Farquhar and Sharkey (Farquhar and Sharkey, 1982) proposed an analysis principle base on stomatal limit value: when photosynthetic rate decreases, if the intercellular CO_2 concentration decreases and the stomatal limit value increases, the decrease of photosynthetic rate is mainly due to stomatal regulation; if the intercellular CO_2 concentration increases and the stomatal limit value

Table 2
Pearson's correlation coefficient between P_n and other parameters of ash and ginkgo (n = 40).

	Tree species	*E*	g_s	C_i	VPD_l	F_v/F_m	Φ_{PSII}	ETR	qP	NPQ
P_n	Ash	0.839**	0.853**	−0.518**	−0.523**	0.346*	0.759**	0.808**	0.586**	−0.752**
	Ginkgo	0.456**	0.580**	−0.746**	−0.307	0.292	0.567**	0.619**	0.606**	0.037

Significance levels: ** $P < 0.01$, * $P < 0.05$. No asterisks mean the absence of a significant relationship.

Table 3
Stepwise regression equations between P_n and other parameters of ash and ginkgo (n = 40).

Tree species	Regression equation	*F* value	R^2	*P*
Ash	$P_n = 1.77\,E - 0.96\,VPD_l - 42.17\,F_v/F_m - 1.84\,NPQ + 44.33$	101.50	0.91	<0.001
Ginkgo	$P_n = 2.67\,E - 0.03\,C_i - 2.00\,VPD_l + 8.60\,\Phi_{PSII} + 11.15$	73.05	0.88	<0.001

decreases, the decrease of photosynthetic rate is mainly caused by non-stomatal regulation. In our study, the D treatment with a decrease in soil moisture of 2.8% or 2.7% and the DP treatment with a decrease in soil moisture of 4.1% or 4.0% for ash or ginkgo, respectively (Fig. 3), could be considered as a mild drought, and also as a chronic drought because the water reduction was sustained for two successive growing seasons. There was a significantly positive correlation between P_n and g_s for both ash and ginkgo (Table 2). This convincingly infers that stomatal regulation exerts important effects on gas exchange for the decrease of g_s that inhibited the P_n and *E*. Furthermore, there was a greater reduction of g_s in DP than in D, which is considered an important reason for the significantly greater down-regulation of P_n in DP than in D. However, the C_i of ash and ginkgo significantly increased in D and DP (Table 1), which fitted the scenario of non-stomatal regulation proposed by Farquhar and Sharkey (1982). Moreover, other gas exchange and chlorophyll fluorescence parameters showed significant relationships with P_n (Table 2). Additionally, *E*, VPD_l, and F_v/F_m have been screened out as main factors influencing P_n by stepwise regression (Table 3), which indicates that non-stomatal regulation for photosynthesis is also very important.

Various photochemical, physiological, and biochemical parameters can be deemed to be complex non-stomatal regulation for photosynthesis. Discussing the corresponding effects on each process of photosynthesis is necessary. Plant photosynthesis mainly consists of three steps: (i) primary reactions; (ii) electron transfer and photophosphorylation; and (iii) carbon assimilation (Pan et al., 2012). Once each step is significantly affected, the photosynthesis/photosynthetic rate would be inevitably altered (Fig. 4). Though this study did not directly measure the related key biochemical parameters, the parameters of chlorophyll fluorescence and the parameters estimated from the light and CO_2 response models based on seasonal and almost nondestructive measurements by the photosynthesis analyzer would be appropriately characterizing the corresponding photosynthesis processes.

The first step is deeply influenced by photosynthetic pigments (Pan et al., 2012). Numerous studies have shown that drought stress and/or heat stress can decrease photosynthetic pigment content (Chl a, Chl b, and Chl (a + b)) significantly (Dias et al., 2018; Guerfel et al., 2009; Semerci et al., 2016; Zhang et al., 2011). However, no parameter involving photosynthetic pigments was directly measured in this study.

In the second step, the photochemistry efficiency and ETR in photosystem II (PSII) are the key parameters which are related to chlorophyll fluorescence parameters including F_v/F_m, Φ_{PSII}, and ETR and J_{max} estimated from CO_2 response curves in this study. Ashraf and Harris (2013) reviewed that drought and high-temperature stress adversely affected the functionality of both photosystems and reduced electron transport through them and that this results in a low production of ATP and NADPH. Generally in healthy leaves, the F_v/F_m value was close to 0.8 in most plant species, therefore a lower value indicates that a proportion of PSII reaction centers is damaged or inactivated, a phenomenon, termed as photoinhibition, commonly observed in plants under stress (Ashraf and Harris, 2013; Ogaya et al., 2011). In our study, there was no significant difference in the F_v/F_m of ash among different treatments (Table 1), and most of the F_v/F_m values of ash appeared very close to 0.8 (the data were not shown), which revealed that ash showed environmental stress stability of the photosynthetic apparatus (Yamori et al., 2014). However, significant decreases in F_v/F_m of ginkgo only in DP in comparison to the control were observed (Table 1), indicating that the photosystem of ginkgo may be damaged or inactivated. Drought and its combination with pavement can also bring adverse effects on the Φ_{PSII}, ETR and J_{max} of both ash and ginkgo. We observed that the Φ_{PSII}, ETR and J_{max} of ash and ginkgo were significantly decreased in D treatment and more in DP treatment as compared with the control (Table 1). Similarly, Robredo et al. (2010) reported that drought treatments caused a slight effect on F_v/F_m and decreased Φ_{PSII} and J_{max} in barley, which could be associated with a down-regulation of PSII during water stress. Additionally, environmental stress can bring changes to the distribution of light energy in photochemical action, thermal dissipation, and fluorescence (Horton and Ruban, 2005), which are characterized by the qP and NPQ. In this study, the qP of ash and ginkgo significantly decreased in D and DP treatments whereas NPQ increased (Table 1), indicating that the absorbed light dissipated more through a thermal reaction and not by using a photochemical reaction in drought and the combination of drought with pavement (Song et al., 2015). In fact, the increase of NPQ is also a mechanism for protecting PSII from photoinhibition (Huang et al., 2013). The significantly negative relationship between NPQ and P_n was only found in ash but not in ginkgo (Table 2), indicating that this protective mechanism may occur only in ash.

In the third step, the carbon assimilation pathway (Calvin cycle) of C_3 plants can be divided into three stages: carboxylation, reduction, and regeneration. Carboxylation efficiency reflects Rubisco content and activity (Pan et al., 2012). Under drought and/or heat stress, decreases in Rubisco content and activity have been found in many previous studies (Nishida and Hanba, 2017; Rennenberg et al., 2006; Yamori et al., 2012). Mechanistically, it has been proposed that the activity of Rubisco activase is insufficient to keep pace with the faster rates of Rubisco inactivation at high temperatures (Yamori et al., 2014). The maximum carboxylation rate (V_{cmax}) is an important parameter characterizing the photosynthetic capacity of plants and determines the maximum net photosynthetic rate, photorespiration, and the mitochondrial respiration process (Farquhar et al., 1980; Wullschleger, 1993). The V_{cmax} of both ash and ginkgo was significantly lower in D treatment than that in the control and the lowest in DP treatment (Table 1), indicating that the photosynthetic enzyme activity of ash and ginkgo was reduced. This result was in accordance with a study by Vaz et al. (2010), which found that photosynthesis was not only limited by stomatal closure but was also down-regulated as a consequence of a decrease in the V_{cmax} and J_{max} in both holm oak and cork oak. Triose phosphates, including glyceraldehyde 3-phosphate (PGA), are products of the reduction phase and serve as renewable material for RuBP in the regeneration phase (Pan et al., 2012). The TPU of ash and ginkgo significantly decreased in D treatment and decreased more in DP treatment (Table 1), demonstrating that RuBP regeneration decreases, which would influence photosynthetic capacity. J_{max}/V_{cmax} reflects the functional balance between electron transfer and Rubisco ability (RuBP regeneration and consumption) (Wullschleger, 1993) and is considered as an important indicator for measuring the nitrogen distribution pattern in the internal photosystem of leaves. The J_{max}/V_{cmax} in P and DP treatments was significantly reduced only for ginkgo (Table 1), indicating that the functional balance between the electron transfer and Rubisco ability of the leaves was broken.

Apart from the three steps of the photosynthesis process, photorespiration is another important process affecting plant photosynthesis. However, the relationship between photorespiration and photosynthesis is very complex. Photorespiration can inhibit photosynthesis by inhibiting RuBP-regeneration-limited net assimilation because of the CO_2 released in photorespiration but also because each oxygenation consumes one RuBP molecule that is then not available for

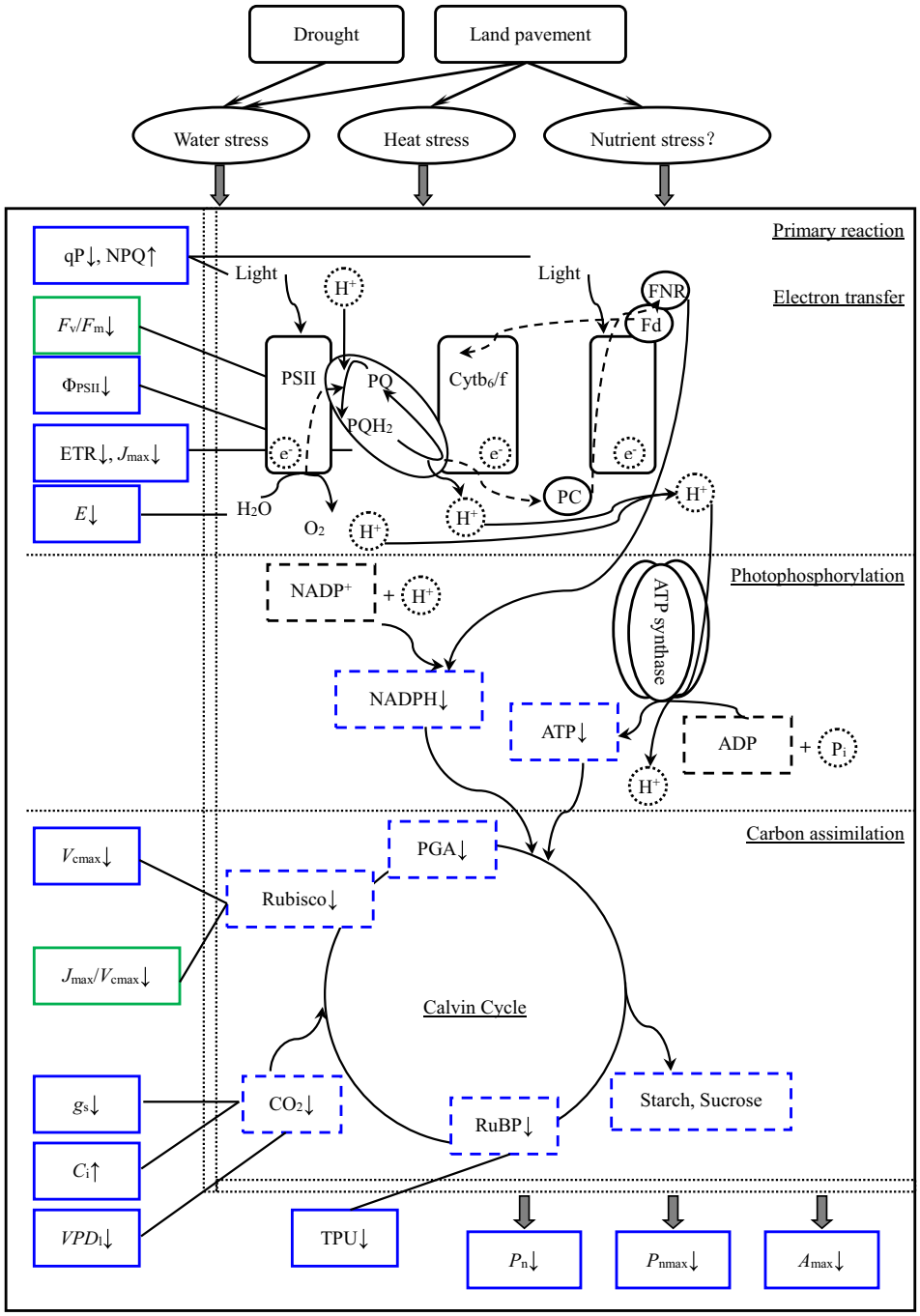

Fig. 4. Impacts of drought and land pavement on photosynthesis processes of ash and ginkgo. Blue border boxes indicate that both ash and ginkgo are affected, green border boxes indicate that only ginkgo is affected. "↓" indicates a decrease, "↑" indicates an increase. (For interpretation of the references to color in this figure legend, the reader is referred to the web version of this article.)

carboxylation (Yang et al., 2016a). Moreover, photorespiration can act with a protective mechanism to avoid a decrease in photosynthesis, such as under conditions of high light and temperature. Photorespiration can consume excess energy to avoid damage to the photosynthetic apparatus and decreases the photosynthetic electron transport rate and light phosphorylation (Noguchi and Yoshida, 2008). The *R*p of ash and ginkgo was significantly lower than the control in D and DP treatments (Table 1). This decrease might inhibit the protection mechanism of photorespiration by using excess energy (Atkin and Macherel, 2009).

Cell osmotic adjustment and reduction in turgor loss point are two other key non-stomatal responses to drought (Bartlett et al., 2012; Hui et al., 2018). In this experiment, it is not measured the parameters related to osmotic adjustment such as proline, soluble sugar, and soluble protein etc. and to turgor loss point such as water potential. It would be necessary in future to investigate the feedback of the responses of osmotic adjustment and turgor loss point to drought and pavement that influences on photosynthesis.

4.4. Difference in the responses of photosynthesis between ash and ginkgo grown on land pavement and in drought

The environmental sensitivity of growth and photosynthesis usually varies among tree species (Jafarnia et al., 2018; Slot et al.,

2016; Teskey et al., 2015) because of the differences in leaf morphology, xylem structure, and physiology (Urban et al., 2017; Wolf et al., 2016). Our study suggested that ginkgo showed more sensitivity to land pavement and drought as compared with ash. In P treatment, P_n, A_{max}, and V_{cmax}, and E significantly decreased for ginkgo but not for ash (Table 1). In DP treatment, F_v/F_m, Rd and J_{max}/V_{cmax} of ginkgo significantly reduced but this was not the case for ash (Table 1). This difference may be attributed to the obvious physiological differences between ash and ginkgo. Ash is ring-porous wood while ginkgo is non-porous wood, the former possesses stronger maximum water transport capacity to ensure water supply better and shows stronger stomatal regulatory ability under water stress (Maherali et al., 2006; Zhang et al., 2015). Moreover, ash exhibits stronger photosynthesis and a higher growth rate than ginkgo which generally appears more flexible to environmental stress. So, ash could be recommended for urban greening on paved land because of its tolerance to urban stress and of high productivity. Although having high ornamental value, ginkgo might not be suitable for planting on paved land because of its sensitivity to drought and hot stresses (Jing et al., 2005; Nie et al., 2015). In Beijing, ginkgo with poor growth or leave yellowing has been widely observed, especially in paved lands such as sidewalk and square (Nie et al., 2015). For urban greening, intolerant trees should be avoided on paved land.

5. Conclusions

Land pavement increases surface and air temperatures and decreases air humidity. The net photosynthetic rate and maximum photosynthetic capacity of ginkgo were significantly inhibited by land pavement. Drought decreased net photosynthetic rate and maximum photosynthetic capacity of both ash and ginkgo and this adverse effect was commonly exacerbated under the combination of drought and pavement, indicating urban trees especially those that are growing on land pavement will confront harsher environment and a greater decline of photosynthesis and growth under the more frequent and severe droughts predicted in the future.

Stomatal regulation (characterized by g_s) exerted key effects on gas exchanges under drought and its combination with land pavement, while the non-stomatal regulation for photosynthesis was also very important. By analyzing the effects of land pavement and drought on photosynthetic processes, the roles of non-stomatal regulation was evident and was shown by parameters such as photochemistry efficiency and electron transfer in PSII (characterized by F_v/F_m, Φ_{PSII}, and ETR and J_{max}), Rubisco content and activity (V_{cmax}), and triose phosphates (TPU). These parameters were significantly reduced under drought treatment and more under its combination with pavement, which resulted in a significant reduction of photosynthetic rates. Overall, ash showed more tolerance to environmental stresses than ginkgo, which indicates that it could contribute to differences in behavior among species in the future climate in cities. To cope with the predicted harsher environment in the future, planting urban tree species with strong environmental tolerance is very important and should be based on further studies on the physiological response and adaptation of urban trees.

Acknowledgements

This work was supported by the National Natural Science Foundation of China (41571035, 71533005) and the National Key Research and Development Program of China (2016YFC0503004). We sincerely thank Ning Yang, Weiwei Yu, Yuanyuan Chen and Yinfu Bai for their help in the field experiment and the reviewers and editors for their suggestions on this paper.

Appendix A

Abbreviations		Abbreviations	
A_{max}	photosynthetic capacity	NPQ	non-photochemical quenching parameter
C_i	intercellular CO_2 concentration	P_n	net photosynthetic rate
C_{isat}	saturated intercellular CO_2 concentration	P_{nmax}	maximum net photosynthetic rate
E	transpiration rate	qP	photochemical quenching parameter
ETR	apparent electron transfer rate	Rd	dark respiration rate
F_v/F_m	maximum quantum yield	Rp	photorespiration rate
g_s	stomatal conductance	TPU	triose phosphate utilization rate
I_c	light compensation point	V_{cmax}	maximum carboxylation rate
I_{sat}	light saturation point	VPD_l	leaf vapor pressure deficit
J_{max}	maximum electron transfer rate	Φ_{PSII}	effective quantum yield
J_{max}/V_{cmax}	ratio between J_{max} and V_{cmax}	Γ	CO_2 compensation point

Appendix B

The modified rectangular hyperbolic model for light intensity response curves can be expressed as follows in Eq. (1) (Ye, 2010)

$$P_n = \alpha \frac{1-\beta\ I}{1+\gamma\ I} I - R_d \tag{1}$$

where P_n is the net photosynthetic rate; I is the photosynthetically active radiation; R_d is the dark respiration rate, which can be calculated directly; α is the initial slope of the light intensity response curve of photosynthesis when the light intensity approaches zero; and β and γ are coefficients that are independent of I. The light compensation point (I_c) is the light intensity when $P_n = 0$, and the maximum net photosynthetic rate (P_{nmax}) and light saturation point (I_{sat}) can be calculated using the formulas in Eqs. (2) and (3):

$$P_{nmax} = \alpha \left(\frac{\sqrt{\beta+\gamma} - \sqrt{\beta}}{\gamma} \right)^2 - R_d \tag{2}$$

$$I_{sat} = \frac{\sqrt{(\beta+\gamma)/\beta} - 1}{\gamma} \tag{3}$$

The modified rectangular hyperbolic model for CO_2 response curves can be expressed as follows in Eq. (4) (Ye, 2010):

$$P_n = a \frac{1-bC_i}{1+cC_i} C_i - R_p \tag{4}$$

where P_n is the net photosynthetic rate; C_i is the intercellular CO_2 concentration; R_p is the photorespiration rate, which can be calculated directly; a is the initial carboxylation efficiency (CE); and b and c are coefficients that are independent of C_i. The CO_2 compensation point (Γ) is the intercellular CO_2 concentration when $P_n = 0$, and the photosynthetic capacity (A_{max}) and saturated intercellular CO_2 concentration (C_{isat}) can be calculated using the formulas in Eqs. (5) and (6):

$$A_{max} = a \left(\frac{\sqrt{b+c} - \sqrt{b}}{c} \right)^2 - R_p \tag{5}$$

$$C_{isat} = \frac{\sqrt{(b+c)/b} - 1}{c} \quad (6)$$

The biochemical model for CO_2 response curves can be expressed as follows in Eq. (7):

$$P_n = \min\{w_c, w_j, w_p\}\left(1 - \frac{\Gamma^*}{C_i}\right) - R_d \quad (7)$$

where P_n is the net photosynthetic rate; w_c, w_j, and w_p represent the potential CO_2 assimilation rate supported by Rubisco activity, RuBP and inorganic phosphate regeneration, respectively; Γ^* is the CO_2 compensation point (excluding dark respiration); C_i is the intercellular CO_2 concentration; and R_d is the dark respiration rate under light. The values of w_c, w_j, and w_p can be expressed as follows in Eqs. (8)–(10) (Ye, 2010):

$$w_c = \frac{V_{c\,max} C_i}{C_i + K_c(1 + O/K_o)} \quad (8)$$

$$w_j = \frac{JC_i}{4.5C_i + 10.5\Gamma^*} \quad (9)$$

$$w_p = \frac{3TPU}{1 - \frac{\Gamma^*}{C_i}} \quad (10)$$

where V_{cmax} is the maximum Rubisco carboxylation rate; J is the electron transfer rate for RuBP regeneration at light saturation, which is equal to J_{max}; TPU is the triose phosphate utilization efficiency; and K_c and K_o are the Michaelis–Menten constants for carboxylation and oxygenation, respectively (Farquhar et al., 1980).

References

Ashraf, M., Harris, P.J.C., 2013. Photosynthesis under stressful environments: an overview. Photosynthetica 51 (2), 163–190.

Atkin, O.K., Macherel, D., 2009. The crucial role of plant mitochondria in orchestrating drought tolerance. Ann. Bot. 103 (4), 581–597.

Balakina, J.N., Makarova, O.V., Bondarenko, V.V., Koudstaal, L.J., Ros, E.J., Koolen, A.J., van Loon, W.K.P., 2005. Simulation of oxygen regime of tree substrates. Urban For. Urban Green. 4 (1), 23–35.

Bartlett, M.K., Scoffoni, C., Sack, L., 2012. The determinants of leaf turgor loss point and prediction of drought tolerance of species and biomes: a global meta-analysis. Ecol. Lett. 15 (5), 393–405.

Berland, A., Shiflett, S.A., Shuster, W.D., Garmestani, A.S., Goddard, H.C., Herrmann, D.L., Hopton, M.E., 2017. The role of trees in urban stormwater management. Landsc. Urban Plan. 162, 167–177.

Bian, G.D., Du, J.K., Song, M.M., Xu, Y.P., Xie, S.P., Zheng, W.L., Xu, C.Y., 2017. A procedure for quantifying runoff response to spatial and temporal changes of impervious surface in Qinhuai River basin of southeastern China. Catena 157, 268–278.

Bolker, B.M., Brooks, M.E., Clark, C.J., Geange, S.W., Poulsen, J.R., Stevens, M.H., White, J.S., 2009. Generalized linear mixed models: a practical guide for ecology and evolution. Trends Ecol. Evol. 24 (3), 127–135.

Breshears, D.D., Myers, O.B., Meyer, C.W., Barnes, F.J., Zou, C.B., Allen, C.D., McDowell, N.G., Pockman, W.T., 2009. Tree die-off in response to global change-type drought: mortality insights from a decade of plant water potential measurements. Front. Ecol. Environ. 7 (4), 185–189.

Chaves, M.M., Flexas, J., Pinheiro, C., 2009. Photosynthesis under drought and salt stress: regulation mechanisms from whole plant to cell. Ann. Bot. 103 (4), 551–560.

Chen, Y., Wang, X., Jiang, B., Yang, N., Li, L., 2016. Pavement induced soil warming accelerates leaf budburst of ash trees. Urban For. Urban Green. 16, 36–42.

Chen, Y., Wang, X., Jiang, B., Wen, Z., Yang, N., Li, L., 2017a. Tree survival and growth are impacted by increased surface temperature on paved land. Landsc. Urban Plan. 162, 68–79.

Chen, Y., Jiang, B., Wang, X., Li, L., 2017b. Effect of pavement on the leaf photosynthetic characteristics of saplings of three common tree species (*Pinus tabuliformis*, *Fraxinus chinensis*, and *Acer truncatum*) in Beijing. Acta Ecol. Sin. 37 (11), 3673–3682 (In Chinese).

Danyagri, G., Dang, Q.-L., 2014. Effects of elevated [CO_2] and soil temperature on photosynthetic responses of mountain maple (*Acer spicatum* L.) seedlings to light. Environ. Exp. Bot. 107, 64–70.

Dias, M.C., Correia, S., Serôdio, J., Silva, A.M.S., Freitas, H., Santos, C., 2018. Chlorophyll fluorescence and oxidative stress endpoints to discriminate olive cultivars tolerance to drought and heat episodes. Sci. Hortic. 231, 31–35.

Douglas, I., 2012. Urban ecology and urban ecosystems: understanding the links to human health and well-being. Curr. Opin. Environ. Sustain. 4 (4), 385–392.

Edmondson, J.L., Davies, Z.G., McHugh, N., Gaston, K.J., Leake, J.R., 2012. Organic carbon hidden in urban ecosystems. Sci. Rep. 2, 963.

Edmondson, J.L., Stott, I., Davies, Z.G., Gaston, K.J., Leake, J.R., 2016. Soil surface temperatures reveal moderation of the urban heat island effect by trees and shrubs. Sci. Rep. 6, 33708.

Escobedo, F.J., Kroeger, T., Wagner, J.E., 2011. Urban forests and pollution mitigation: analyzing ecosystem services and disservices. Environ. Pollut. 159 (8–9), 2078–2087.

Ethier, G.J., Livingston, N.J., 2004. On the need to incorporate sensitivity to CO_2 transfer conductance into the Farquhar-von Caemmerer-Berry leaf photosynthesis model. Plant Cell Environ. 27, 137–153.

Farooq, M., Wahid, A., Kobayashi, N., Fujita, D., Basra, S.M.A., 2009. Plant drought stress: effects, mechanisms and management. Agron. Sustain. Dev. 29 (1), 185–212.

Farquhar, G.D., Sharkey, T.D., 1982. Stomatal conductance and photosynthesis. Annu. Rev. Plant Physiol. 33, 317–345.

Farquhar, G.D., von Caemmerer, S., Berry, J.A., 1980. A biochemical model of photosynthetic CO_2 assimilation in leaves of C_3 species. Planta 149 (1), 78–90.

Ghosh, S., Scharenbroch, B.C., Burcham, D., Ow, L.F., Shenbagavalli, S., Mahimairaja, S., 2016. Influence of soil properties on street tree attributes in Singapore. Urban Ecosyst. 19 (2), 949–967.

Gilbert, M.E., Zwieniecki, M.A., Holbrook, N.M., 2011. Independent variation in photosynthetic capacity and stomatal conductance leads to differences in intrinsic water use efficiency in 11 soybean genotypes before and during mild drought. J. Exp. Bot. 62 (8), 2875–2887.

Grimm, N.B., Faeth, S.H., Golubiewski, N.E., Redman, C.L., Wu, J., Bai, X., Briggs, J.M., 2008. Global change and the ecology of cities. Science 319 (5864), 756–760.

Guerfel, M., Baccouri, O., Boujnah, D., Chaïbi, W., Zarrouk, M., 2009. Impacts of water stress on gas exchange, water relations, chlorophyll content and leaf structure in the two main Tunisian olive (*Olea europaea* L.) cultivars. Sci. Hortic. 119 (3), 257–263.

Guo, P., Su, Y., Wan, W., Liu, W., Zhang, H., Sun, X., Ouyang, Z., Wang, X., 2018. Urban plant diversity in relation to land use types in built-up areas of Beijing. Chin. Geogr. Sci. 28 (1), 100–110.

Hagishima, A., 2018. Green Infrastructure and Urban Sustainability. 1927 p. 020002.

Horton, P., Ruban, A., 2005. Molecular design of the photosystem II light-harvesting antenna: photosynthesis and photoprotection. J. Exp. Bot. 56 (411), 365–373.

Hothorn, T., Bretz, F., Westfall, P., 2008. Simultaneous inference in general parametric models. Biom. J. 50 (3), 346–363.

Huang, W., Fu, P.L., Jiang, Y.J., Zhang, J.L., Zhang, S.B., Hu, H., Cao, K.F., 2013. Differences in the responses of photosystem I and photosystem II of three tree species *Cleistanthus sumatranus*, *Celtis philippensis* and *Pistacia weinmannifolia* exposed to a prolonged drought in a tropical limestone forest. Tree Physiol. 33 (2), 211–220.

Hui, R., Zhao, R., Song, G., Li, Y., Zhao, Y., Wang, Y., 2018. Effects of enhanced ultraviolet-B radiation, water deficit, and their combination on UV-absorbing compounds and osmotic adjustment substances in two different moss species. Environ. Sci. Pollut. Res. Int. 25 (15), 14953–14963.

Jafarnia, S., Akbarinia, M., Hosseinpour, B., Modarres Sanavi, S.A.M., Salami, S.A., 2018. Effect of drought stress on some growth, morphological, physiological, and biochemical parameters of two different populations of *Quercus brantii*. iForest Biogeosci. For. 11 (2), 212–220.

Jamil, T., Ozinga, W.A., Kleyer, M., Braak, C.J., 2013. Selecting traits that explain species–environment relationships: a generalized linear mixed model approach. J. Veg. Sci. 24, 988–1000.

Jing, M., Cao, F., Wang, G., Hao, M., 2005. The effects of soil water contents on photosynthetic characteristics of ginkgo. J. Nanjing Forest. Univ. (Nat. Sci. Ed.) 29 (4), 83–86 (In Chinese).

Kashiwagi, J., Morito, Y., Jitsuyama, Y., An, P., Inoue, T., Inagaki, M., 2015. Effects of root water uptake efficiency on soil water utilization in wheat (*Triticum aestivum* L.) under severe drought environments. J. Agron. Crop Sci. 201 (3), 161–172.

Kjelgren, R., Montague, T., 1998. Urban tree transpiration over turf and asphalt surfaces. Atmos. Environ. 32 (1), 35–41.

Kuang, W., Liu, J., Zhang, Z., Lu, D., Xiang, B., 2012. Spatiotemporal dynamics of impervious surface areas across China during the early 21st century. Chin. Sci. Bull. 58 (14), 1691–1701.

Leuzinger, S., Vogt, R., Körner, C., 2010. Tree surface temperature in an urban environment. Agric. For. Meteorol. 150 (1), 56–62.

Liu, J., Deng, X., 2011. Impacts and mitigation of climate change on Chinese cities. Curr. Opin. Environ. Sustain. 3 (3), 188–192.

Maherali, H., Moura, C.F., Caldeira, M.C., Willson, C.J., Jackson, R.B., 2006. Functional coordination between leaf gas exchange and vulnerability to xylem cavitation in temperate forest trees. Plant Cell Environ. 29 (4), 571–583.

Margaritis, E., Kang, J., 2017. Relationship between green space-related morphology and noise pollution. Ecol. Indic. 72, 921–933.

McClung, T., Ibáñez, I., 2018. Quantifying the synergistic effects of impervious surface and drought on radial tree growth. Urban Ecosyst. 21 (1), 147–155.

Moser, A., Rahman, M.A., Pretzsch, H., Pauleit, S., Rotzer, T., 2017a. Inter- and intraannual growth patterns of urban small-leaved lime (*Tilia cordata* mill.) at two public squares with contrasting microclimatic conditions. Int. J. Biometeorol. 61 (6), 1095–1107.

Moser, A., Uhl, E., Rötzer, T., Biber, P., Dahlhausen, J., Lefer, B., Pretzsch, H., 2017b. Effects of climate and the urban heat island effect on urban tree growth in Houston. Open J. For. 07 (04), 428–445.

Moualeu-Ngangue, D.P., Chen, T.W., Stutzel, H., 2017. A new method to estimate photosynthetic parameters through net assimilation rate-intercellular space CO_2 concentration (A-C_i) curve and chlorophyll fluorescence measurements. New Phytol. 213 (3), 1543–1554.

Mueller, E.C., Day, T.A., 2005. The effect of urban ground cover on microclimate, growth and leaf gas exchange of oleander in Phoenix, Arizona. Int. J. Biometeorol. 49 (4), 244–255.
Mullaney, J., Trueman, S.J., Lucke, T., Bai, S.H., 2015. The effect of permeable pavements with an underlying base layer on the ecophysiological status of urban trees. Urban For. Urban Green. 14 (3), 686–693.
Mullerova, J., Vitkova, M., Vitek, O., 2011. The impacts of road and walking trails upon adjacent vegetation: effects of road building materials on species composition in a nutrient poor environment. Sci. Total Environ. 409 (19), 3839–3849.
Nakagawa, S., Schielzeth, H., 2013. A general and simple method for obtaining R^2 from generalized linear mixed-effects models. Methods Ecol. Evol. 4 (2), 133–142.
Nie, Q., Wang, Y., Wang, M., Cong, R., 2015. The growth of ginkgo in summer and ite relationship with the meteorological and site environment. Beijing Gard. 31 (3), 39–52 (In Chinese).
Nishida, K., Hanba, Y.T., 2017. Photosynthetic response of four fern species from different habitats to drought stress: relationship between morpho-anatomical and physiological traits. Photosynthetica 55 (4), 689–697.
Noguchi, K., Yoshida, K., 2008. Interaction between photosynthesis and respiration in illuminated leaves. Mitochondrion 8 (1), 87–99.
Ogaya, R., Peñuelas, J., Asensio, D., Llusià, J., 2011. Chlorophyll fluorescence responses to temperature and water availability in two co-dominant Mediterranean shrub and tree species in a long-term field experiment simulating climate change. Environ. Exp. Bot. 73, 89–93.
Oleson, K.W., Monaghan, A., Wilhelmi, O., Barlage, M., Brunsell, N., Feddema, J., Hu, L., Steinhoff, D.F., 2013. Interactions between urbanization, heat stress, and climate change. Clim. Chang. 129 (3–4), 525–541.
Pan, R.Z., Wang, X.J., Li, N.H., 2012. Plant Physiology. Higher Education Press, Beijing, China, pp. 69–119 (In Chinese).
Qin, H.P., Li, Z.X., Fu, G., 2013. The effects of low impact development on urban flooding under different rainfall characteristics. J. Environ. Manag. 129, 577–585.
R Development Core Team, 2018. R: a language and environment for statistical computing. Version 3.5.0. R Foundation for Statistical Computing, Vienna, Austria.
Rantzoudi, E.C., Georgi, J.N., 2017. Correlation between the geometrical characteristics of streets and morphological features of trees for the formation of tree lines in the urban design of the city of Orestiada, Greece. Urban Ecosyst. 20 (5), 1081–1093.
Reichstein, M., Bahn, M., Ciais, P., Frank, D., Mahecha, M.D., Seneviratne, S.I., Zscheischler, J., Beer, C., Buchmann, N., Frank, D.C., Papale, D., Rammig, A., Smith, P., Thonicke, K., van der Velde, M., Vicca, S., Walz, A., Wattenbach, M., 2013. Climate extremes and the carbon cycle. Nature 500 (7462), 287–295.
Rennenberg, H., Loreto, F., Polle, A., Brilli, F., Fares, S., Beniwal, R.S., Gessler, A., 2006. Physiological responses of forest trees to heat and drought. Plant Biol. (Stuttg.) 8 (5), 556–571.
Robredo, A., Pérez-López, U., Lacuesta, M., Mena-Petite, A., Muñoz-Rueda, A., 2010. Influence of water stress on photosynthetic characteristics in barley plants under ambient and elevated CO_2 concentrations. Biol. Plant. 54 (2), 285–292.
Sanesi, G., Colangelo, G., Lafortezza, R., Calvo, E., Davies, C., 2016. Urban green infrastructure and urban forests: a case study of the Metropolitan Area of Milan. Landsc. Res. 42 (2), 164–175.
Savi, T., Bertuzzi, S., Branca, S., Tretiach, M., Nardini, A., 2015. Drought-induced xylem cavitation and hydraulic deterioration: risk factors for urban trees under climate change? New Phytol. 205 (3), 1106–1116.
Schule, S.A., Gabriel, K.M.A., Bolte, G., 2017. Relationship between neighbourhood socioeconomic position and neighbourhood public green space availability: an environmental inequality analysis in a large German city applying generalized linear models. Int. J. Hyg. Environ. Health 220 (4), 711–718.
Semerci, A., Semerci, H., Çalişkan, B., Çiçek, N., Ekmekçi, Y., Mencuccini, M., 2016. Morphological and physiological responses to drought stress of European provenances of Scots pine. Eur. J. For. Res. 136 (1), 91–104.
Slot, M., Garcia, M.N., Winter, K., 2016. Temperature response of CO_2 exchange in three tropical tree species. Funct. Plant Biol. 43 (5), 468–478.
Song, Y., Li, F., Wang, X., Xu, C., Zhang, J., Liu, X., Zhang, H., 2015. The effects of urban impervious surfaces on eco-physiological characteristics of Ginkgo biloba: a case study from Beijing, China. Urban For. Urban Green. 14 (4), 1102–1109.
Teskey, R., Wertin, T., Bauweraerts, I., Ameye, M., McGuire, M.A., Steppe, K., 2015. Responses of tree species to heat waves and extreme heat events. Plant Cell Environ. 38 (9), 1699–1712.
Urban, J., Ingwers, M.W., McGuire, M.A., Teskey, R.O., 2017. Increase in leaf temperature opens stomata and decouples net photosynthesis from stomatal conductance in *Pinus taeda* and *Populus deltoides* × *nigra*. J. Exp. Bot. 68 (7), 1757–1767.
Vaz, M., Pereira, J.S., Gazarini, L.C., David, T.S., David, J.S., Rodrigues, A., Maroco, J., Chaves, M.M., 2010. Drought-induced photosynthetic inhibition and autumn recovery in two Mediterranean oak species (*Quercus ilex* and *Quercus suber*). Tree Physiol. 30 (8), 946–956.
Weissert, L.F., Salmond, J.A., Schwendenmann, L., 2016. Photosynthetic CO_2 uptake and carbon sequestration potential of deciduous and evergreen tree species in an urban environment. Urban Ecosyst. 20 (3), 663–674.
Weng, Q., 2012. Remote sensing of impervious surfaces in the urban areas: requirements, methods, and trends. Remote Sens. Environ. 117, 34–49.
Wolf, A., Anderegg, W.R., Pacala, S.W., 2016. Optimal stomatal behavior with competition for water and risk of hydraulic impairment. Proc. Natl. Acad. Sci. U. S. A. 113 (46), E7222–E7230.
Wullschleger, S.D., 1993. Biochemical limitations to carbon assimilation in C_3 plants-a retrospective analysis of the A_Ci curves from 109. J. Exp. Bot. 44, 907–920.
Xu, Z., Zhou, G., Shimizu, H., 2014. Plant responses to drought and rewatering. Plant Signal. Behav. 5 (6), 649–654.
Yamori, W., Masumoto, C., Fukayama, H., Makino, A., 2012. Rubisco activase is a key regulator of non-steady-state photosynthesis at any leaf temperature and, to a lesser extent, of steady-state photosynthesis at high temperature. Plant J. 71 (6), 871–880.
Yamori, W., Hikosaka, K., Way, D.A., 2014. Temperature response of photosynthesis in C_3, C_4, and CAM plants: temperature acclimation and temperature adaptation. Photosynth. Res. 119 (1–2), 101–117.
Yang, J.T., Preiser, A.L., Li, Z., Weise, S.E., Sharkey, T.D., 2016a. Triose phosphate use limitation of photosynthesis: short-term and long-term effects. Planta 243 (3), 687–698.
Yang, N., Wang, X., Cotrozzi, L., Chen, Y., Zheng, F., 2016b. Ozone effects on photosynthesis of ornamental species suitable for urban green spaces of China. Urban For. Urban Green. 20, 437–447.
Yang, J., Sun, J., Ge, Q., Li, X., 2017. Assessing the impacts of urbanization-associated green space on urban land surface temperature: a case study of Dalian, China. Urban For. Urban Green. 22, 1–10.
Ye, Z.P., 2010. A review on modeling of responses of photosynthesis to light and CO_2. Chin. J. Plant Ecol. 34 (6), 727–740 (In Chinese).
You, H.N., Woo, S.Y., Park, C.R., 2016. Physiological and biochemical responses of roadside trees grown under different urban environmental conditions in Seoul. Photosynthetica 54 (3), 478–480.
Zhang, Y.J., Xie, Z.K., Wang, Y.J., Su, P.X., An, L.P., Gao, H., 2011. Effect of water stress on leaf photosynthesis, chlorophyll content, and growth of oriental lily. Russ. J. Plant Physiol. 58 (5), 844–850.
Zhang, J., He, Q., Shi, W., Otsuki, K., Yamanaka, N., Du, S., 2015. Radial variations in xylem sap flow and their effect on whole-tree water use estimates. Hydrol. Process. 29 (24), 4993–5002.